PREDICTION OF DELAMINATION STRENGTH AT INTERFACE BETWEEN THIN FILM AND SUBSTRATE BY COHESIVE ZONE MODEL

DO VAN TRUONG[1,2], HIROYUKI HIRAKATA[1] AND TAKAYUKI KITAMURA[1]

[1] *Department of Engineering Physics and Mechanics, Kyoto University, Japan*

[2] *Department of Design of Machinery & Robot,*
Hanoi University of Technology, Vietnam

Email: dovantruong@yahoo.com

Abstract. An electronic device consists of multi-layered submicron-thick films, and delamination often takes place at an interface edge because of the stress singularity near the edge. Since the stress singularity at an interface edge depends on the edge shape, the fracture mechanics concept cannot be used to compare the delamination strength between the components with different shapes. This paper aims to predict the delamination strength at the interface edge with arbitrary shape using a cohesive zone model. Two different experiments are conducted for a gold thin film on a silicon substrate to calibrate the cohesive law. The validity of the approach is then discussed.

1. INTRODUCTION

Delamination is one of the mechanical failures often met in microelectronic devices and it sometimes brings about fatal malfunction of the system. Therefore, the quantitative comparison of interface strength between bi-materials of different combinations is a necessary task to choose the suitable materials and improve the reliability of the devices.

In terms of mechanical strength, delamination is mainly caused by the concentrated stress near the interface edge due to the mismatch of the elastic property. According to Bogy [1], the stress field near the interface edge is expressed by the following equation

$$\sigma = \frac{K}{r^\lambda} \tag{1.1}$$

here, K is the stress intensity parameter, r is the distance from the edge and λ is the stress singularity. Crack initiation is governed by the singular stress field and the strength is characterized by K [2-5]. The criterion of crack initiation is described using K as,

$$K = K_c \tag{1.2}$$

where K_c is the critical stress intensity parameter which is characteristic for each interface edge. However, because the dimension of K, MPa.m$^{-\lambda}$, depends on the stress singularity, λ, namely the material combination and the edge shape, we cannot use K_c to compare the crack initiation strength between different material combinations and between different edge shapes even in the same material combination.

Recently, the cohesive zone model approach has emerged as a powerful tool to simulate the fracture behavior [7-14] with an emphasized feature as removing the singularity

by considering a cohesive zone ahead of a crack tip [15]. In the cohesive zone, the cohesive traction is related to the separation displacement under the cohesive law evaluated by fitting experimental data. The parameters of the cohesive law are specific values to materials (interfaces). By using a cohesive zone approach, we might evaluate the ad hoc interface strength of bi-materials and compare the strength between them.

In this study, the method for evaluating the crack initiation strength from interface edges between thin films and substrates using a cohesive zone model is developed. The cohesive law for an interface between a gold (Au) thin film and a silicon (Si) substrate is calibrated by crack initiation and propagation tests. Then, the crack initiation strength at the interface edges with different shapes are estimated by finite element method (FEM) with the cohesive zone. Finally, the interface strength between different materials is quantitatively compared on the basis of the crack initiation stress

2. EXPERIMENTAL PROCEDURE

2.1. Materials and specimen

Fig. 1 shows a cross-section of a tested material combination. An Au film with the thickness of 200 nm is deposited on a Si substrate of thickness 500 μm by the evaporation method under a pressure of 1.9×10^{-3} Pa. Two different edge angles of 180°/180° (Type A) and 90°/90° (Type B) as shown in Fig. 2 are prepared to calibrate the parameters of the cohesive law.
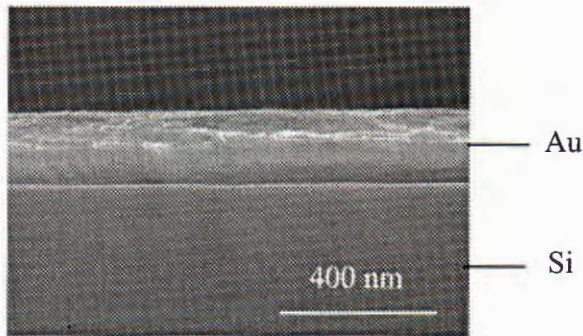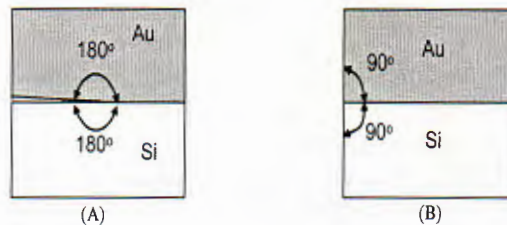

Fig. 1. Cross-section of a test material Au/Si

Fig. 2. Edge shape of interface. Type A with the edge angle of 180°/180°. Type B with the edge angle of 90°/90°

Detail of A

Cantilever

Epoxy (thickness: 10~20 μm)

Thin film, Au

Substrate, Si

Type B (without crack)

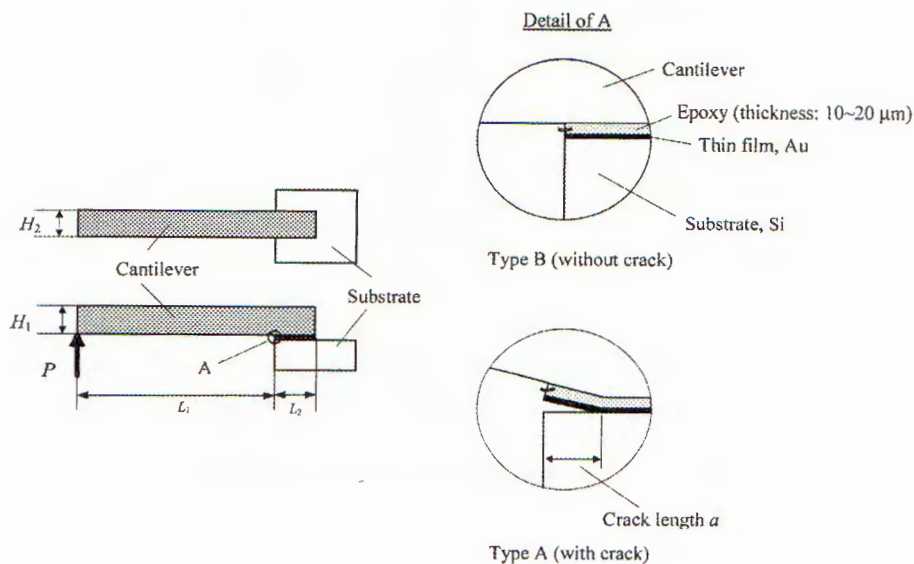Crack length *a*

Type A (with crack)
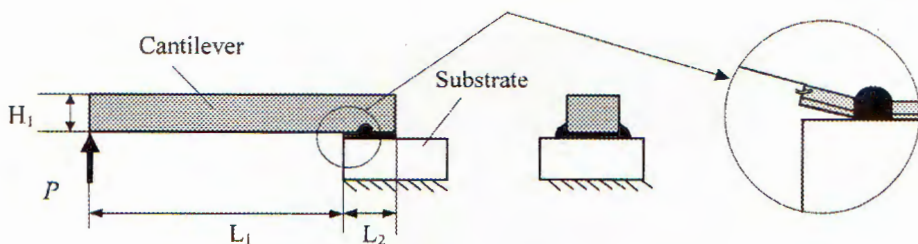
Fig. 3. Specimens and loading system

Fig. 4. Crack initiation

Fig. 3 shows the specimens of Type A and Type B and the loading system. A square coupon is cut from a plate of the material with the Au film and the Si substrate. A cantilever of stainless steel with a polished surface is glued on the coupon by standard epoxy. Then, the Au film outside of the glue region is removed for avoiding the effect of film fracture during the test. For Type A specimens, a pre-crack is introduced by the following method shown in Fig. 4. The substrate and the cantilever are fixed together by a drop of epoxy. Then, a load is applied to the cantilever edge. At a low load, a crack is initiated at the left edge of the interface and stops at the point of the drop. Finally, the drop of epoxy is carefully removed from the specimen. Two and three specimens are prepared for Type A and Type B, respectively, to check the repeatability and the sizes of the specimens are listed in Table 1.

Crack propagation and initiation tests are conducted for the specimens A and B by a remodelled micro-Vickers hardness tester (Shimadzu; MCTE-500). The load, P, is applied at the end of the cantilever at a constant loading rate of 0.02 N/s by an electro-magnetic

Table 1. Specimen sizes and critical loads

		L_1 (mm)	L_2 (mm)	H_1 (mm)	H_2 (mm)	Pre-crack length a (mm)	Critical load P_c, N
Type A	A-1	6.21	5.91	0.96	1.96	2.70	0.50
	A-2	7.01	5.48	0.96	1.87	1.40	0.47
Type B	B-1	8.18	1.70	0.98	2.10	0	0.59
	B-2	7.36	2.31	0.98	1.94	0	0.74
	B-3	8.83	1.93	0.97	2.07	0	0.55

actuator which is connected to a loading tip with a cone shape, and the displacement at the loading point, u_y, is monitored during the test. All the tests are conducted at a room temperature in laboratory air.

2.2. Experiment results

In all the tests, the relationship between P and u_y is almost linear. At the critical value, P_c, at which u_y remarkably increases, the crack begins to propagate in Type A tests or a crack is initiated at the interface edge in Type B tests along the interface between the Au film and the Si substrate. The resulted critical loads P_c of all the specimens are listed in Table 1.

After the tests, the facture surfaces of both the film and substrate sides are examined by Auger electron spectroscopy. Figures 5 (a) and (b) show the spectra on the film and the substrate sides of a Type B specimen. Only Au peaks (69, 2024 and 2111 eV) are confirmed on the film side while Si peaks (92 and 1619 eV) are recognized on the substrate side. This indicates that the delamination occurs at the clear interface between Au and Si. For the other specimens, the similar spectra are observed.
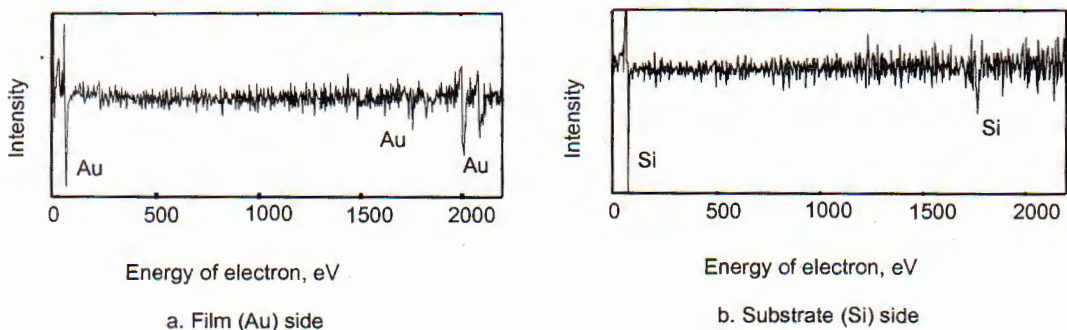

a. Film (Au) side

b. Substrate (Si) side

Fig. 5. Auger electron spectra on the fracture surfaces of Au/Si

3. COHESIVE ZONE MODEL APPROACH

3.1. Idea of the approach

The cohesive zone approach is proposed to remove the singularity by considering a cohesive zone ahead of a crack in which the atomic attraction acts between the separating surfaces. The traction σ in the zone is assumed as a function of the separation distance δ and this relationship is considered as a cohesive law. The work of the interface separation per unit area, Γ_o, is calculated as follows.

$$\Gamma_o = \int_0^{\delta_m} \sigma(\delta) d\delta \tag{3.1}$$

Here, δ_m is the critical separation distance corresponding with the vanishment of traction. For an interface with a specific cohesive law, for example a bi-linear cohesive law shown in Fig. 6, the parameters of Γ_o, δ_m and σ_m (the maximum traction) are specific values to the interface and can be considered like material constants.

3.2. Cohesive zone in finite element analysis

On the basis of the above idea, Needleman [7] introduced the cohesive surface concept in the FEM, in which the predicted crack growth path is inserted by a layer as a cohesive zone. The material behavior in this zone is described by a cohesive law that relates the cohesive traction to the separation displacement between the upper and lower cohesive surfaces. The crack growth occurs only when the separation displacement at the tail of the cohesive zone reaches a critical value, at which the cohesive traction vanishes.

There are many proposed cohesive laws such as bi-linear [11-13], trapezoidal [10, 12] and exponential [16] laws. In this study, the bi-linear cohesive law as shown in Fig. 6 is chosen. The bi-linear cohesive law is characterized by four parameters as the work of interface separation per unit area, Γ_o, the maximum traction σ_m, the maximum separation displacement δ_m, and the initial slope, c. Γ_o can be set at the value equal to the critical energy release rate Γ_c (or critical J-integral, J_c) for an interface crack (edge angle: 180°/180°) in a elastic bi-materials [17], while the other parameters are evaluated by fitting the critical load obtained by the numerical analysis to that obtained by the experiment.
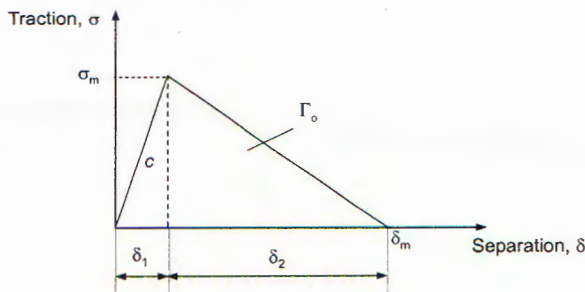

Fig. 6. Bi-linear cohesive law

To eliminate the effect of the thickness of the cohesive layer on the result, the value of thickness is set at one unit length in the FEM [18]. This choice ensures that the strains are equal to the relative separation displacements in the cohesive zone. Kitamura [19] indicated that the stress concentrated region near the interface edge between the Au thin

film and the Si substrate is on the order of 10 nm. Thus, the smallest size of the cohesive element near the interface edge is set at 10 nm in the FEM.

4. CALIBRATION OF THE PARAMETERS OF THE COHESIVE LAW

The cohesive law shown in Fig. 6 can be expressed by a following relationship.

$$\Gamma_o = \frac{1}{2}\sigma_m\delta_m = \frac{1}{2}\sigma_m(\delta_1 + \delta_2) \tag{4.1}$$

or

$$\Gamma_o = \frac{1}{2}\sigma_m\left(\frac{\sigma_m}{c} + \delta_2\right) \tag{4.2}$$

Among the four parameters, only three of them, for example Γ_o, σ_m, and c, are dependent because δ_2 can be obtained from Eq. (5).
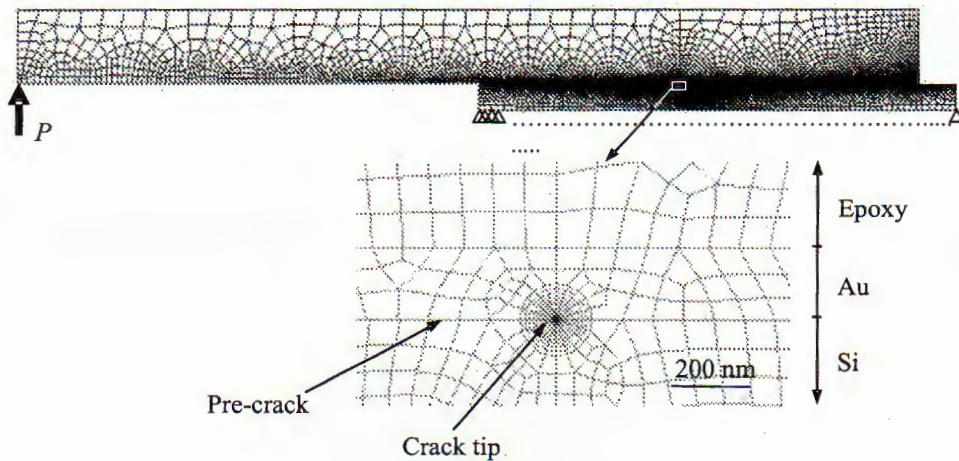

Fig. 7. Mesh division for FEM analysis

The calibration process of the parameters of the cohesive law in Type A is started by a following scheme. The work of the interface separation per unit area Γ_o is set at the value equal to the critical J-integral, J_c. This is justified by the lack of occurred plasticity anywhere in the specimen (in this case, $\Gamma_c = J_c$). J_c is calculated by a commercial FEM code, ABAQUS 6.5, under the plane strain condition. The FEM mesh is shown in Fig. 7, in which a ring of collapsed quadratic quadrilateral elements is used at the crack tip. The critical load, P_c, obtained from the experiment is applied to the edge of the cantilever. The materials are assumed to be linear elastic and isotropic, and the elastic constants used are listed in Table 2. The obtained values of J_c in each specimen are listed in Table 3, and Γ_o is set at the average value of $J_c = 0.165$ J/m^2.

Next, the other parameters σ_m and c are calibrated in the FEM with the cohesive zone. Because the initial slope, c, is insensitive to G_o in the range of from 10^6 GPa/m to 10^8 GPa/m, c is chosen at 10^7 GPa/m in this study. The last parameter, the maximum traction, s_m, is calibrated at 1.0 MPa which is the best match to the measured delamination

Table 2. Elastic constants used in FEM analysis

Material	Si	Au	Epoxy	Stainless steel
Young's modulus E, GPa	167	83	2.5	200
Poisson's ratio ν	0.30	0.44	0.30	0.30

Table 3. Critical J-integral value

Specimen	A-1	A-2
Critical J-integral J_c, J/m^2	0.150	0.180
Average value of J_c, J/m^2	0.165	

load. Therefore, the parameters Γ_o, c and σ_m of the interface Au/Si are successfully calibrated at 0.165 J/m^2, 10^7 GPa/m and 1.0 MPa, respectively.
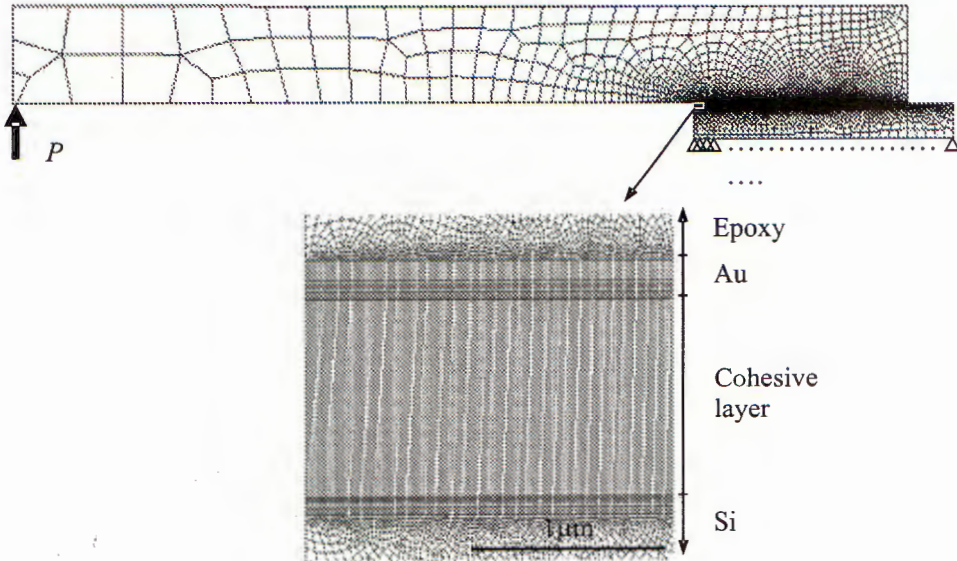

Fig. 8. Mesh division for FEM analysis

The parameters of the cohesive law calibrated above are then validated by the Type B results. Fig. 8 shows the FEM model of a Type B specimen in which the cohesive zone is inserted between the Au film and the Si substrate as a single layer of cohesive elements. The crack initiation load is evaluated when the first cohesive element fails. The crack initiation loads obtained from the cohesive zone approach and from the experiments are listed in Table 4. Both the results agree fairly well with each other. This signifies that the parameters of the cohesive law calibrated for the Au/Si interface are valid and we can ad hoc evaluate the crack initiation load for the interface edge with arbitrary edge shape using the cohesive zone approach.

Table 4. Crack initiation load

Specimen	B-1	B-2	B-3
P_c^{ex}, N	0.59	0.55	0.74
P_c^{CZM}, N	0.52	0.51	0.80

5. CRACK INITIATION STRENGTH

5.1. Comparison of the crack initiation strength among different edge shapes

In this section, the comparison of the crack initiation strengths for the interface edges with different angles on the basis of the cohesive zone model approach. Fig. 9 shows the FEM models of Au interconnects on Si substrates with the edge angles of 60°/180°, 90°/180° and 120°/180°. The bottom face of the Si substrate is completely fixed and the symmetry boundary condition is applied on the right face. Uniform gross stress, σ_g, is applied on the upper surface of the Au part and is monotonically increased. The crack initiation stress, σ_{gc}, is evaluated when the first cohesive element fails. The obtained crack initiation stresses are listed in Table 5. The model with the larger angle of the Au edge has the lower crack initiation strength.
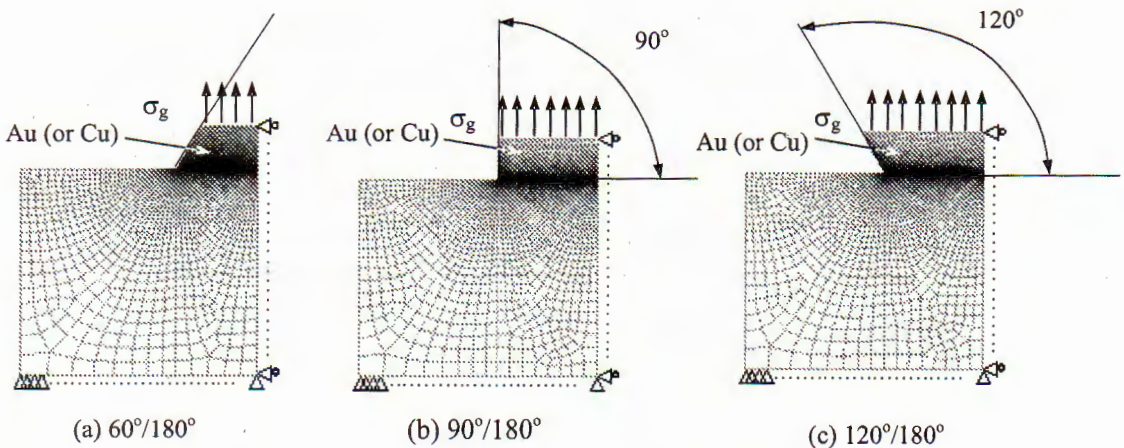

(a) 60°/180°　　(b) 90°/180°　　(c) 120°/180°

Fig. 9. FEM models of Au/Si (Cu/Si) bi-materials with different edge angles

Table 5. Crack initiation stress of Au/Si interface edge

Edge angle	Crack initiation stress σ_{gc}, MPa
60°/180°	2.3
90°/180°	2.0
120°/180°	1.2

5.2. Comparison of the crack initiation strengths for different bi-materials

The crack initiation strength is compared for two different bi-materials. The experimental result for a sputtered copper (Cu) thin film on a Si substrate reported by Hirakata

et al. [20] is used as the counterpart. In this experiment, almost the same specimen and the loading system as the Type A test in the present study were used. The sizes and the critical loads at the crack propagation of two specimens are listed in Table 6. The parameters of the cohesive law of the Cu/Si bi-material are evaluated by the cohesive zone model approach presented above. The elastic constants used are listed in Table 7. The values of Γ_o, c and σ_m are 0.970 J/m^2, 10^7GPa/m and 5.0 MPa, respectively. The crack initiation stresses of the Cu/Si interface edges of $60°/180°$, $90°/180°$ and $120°/180°$ are evaluated by the same manner as that used for the Au/Si interface edges and the results are listed in Table 8. The results indicate the similar tendency to the Au/Si models that the model with the larger angle of the Cu edge has the lower crack initiation strength. Because the specimen geometry is the same for each combination, the crack initiation strength can be quantitatively compared. The strength of the Cu/Si with the angle of $60°/180°$ is 7.4 times higher than that of the Au/Si. The strength of the Cu/Si with the angles of $90°/180°$ and $120°/180°$ is 5.0 and 4.7 times higher than that of the Au/Si, respectively. The difference in the crack initiation strength between the Au/Si and Cu/Si is larger for the smaller edge angle.

Table 6. Specimen sizes of bi-material Cu/Si

	L_1 (mm)	L_2 (mm)	H_1 (mm)	H_2 (mm)	Pre-crack length a (mm)	Critical P_c, N
Type A	10	2.22	1.8	2	0.51	1.36
	10	2.69	1.8	2	0.68	1.46

Table 7. Elastic constants used in FEM analysis

Material	Si	Au	Epoxy	Stainless steel
Young's modulus E, GPa	167	Cu	2.5	200
Poisson's ratio ν	0.30	0.34	0.30	0.30

Table 8. Crack initiation stress of Cu/Si interface edge

Edge angle	Crack initiation stress σ_{gc}, MPa
$60°/180°$	17.0
$90°/180°$	10.0
$120°/180°$	5.6

6. CONCLUSION

A method for evaluating the crack initiation strength from interface edges between thin films and substrates using a cohesive zone model is developed.

The parameters of the cohesive law for a gold (Au) thin film and silicon (Si) substrate are calibrated by crack propagation tests along the interface. The crack initiation loads obtained from the cohesive zone approach and from crack initiation experiments agree fairly well with each other. This signifies the validity of the cohesive law model.

The crack initiation stresses at the interface edges with different shapes are estimated on the basis of the cohesive zone approach. The model with the larger angle of the Au edge has the lower crack initiation strength.

The interface strength of the Au/Si is quantitatively compared with a different bi-material of a sputtered copper (Cu) on a Si substrate by the cohesive zone model approach. The strength of the Cu/Si with the angle of $60°/180°$, $90°/180°$ and $120°/180°$ is 7.4, 5.0 and 4.7 times higher than that of the Au/Si, respectively. The difference in the crack initiation strength between the Au/Si and the Cu/Si is larger for the smaller edge angle.

REFERENCES

1. D. B. Bogy, Edge bonded dissimilar orthogonal elastic wedges under normal and shear stress, *J. Appl. Mech.* **35** (1968) 146–54

2. H. Hirakata, T. Kitamura, Y. Yamamoto, Evaluation of interface strength of micro-dot on substrate by means of AFM, *Int. J. Solids Struct.* **41** (2004) 3243.

3. T. Kitamura, H. Hirakata, T. Itsuji, Effect of residual stress on delamination from interface edge between nano-films, *Engng. Fract. Mech.* **70** (2003) 2089.

4. T. Kitamura, T. Shibutani, T. Ueno, Crack initiation at free edge of interface between thin films in advanced LSI, *Engng. Fract. Mech.* **69** (2002) 1289–99.

5. F. Shang, T. Kitamura, H. Hirakata, I. Kanno, H. Kotera, K. Terada, Experimental and theoretical investigations of delamination at free edge of interface between piezoelectric thin films on a substrate, *Int. J. Solids Struct.* **42** (2005) 1729.

6. C. F. Shih., R. J. Asaro, Elastic-plastic analysis pf cracks on bi-material interfaces: Part I-Small scale yielding, *J. Applied Mech.* **55** (1998) 299-316.

7. A. Needleman, A continuum model for void nucleation by inclusion debonding, *ASME Journal of Applied Mechanics* **54** (1987) 525–531.

8. V. Tvergaard, Effect of strain-dependent cohesive zone model on predictions of crack growth resistance, *J. Solid Structures* **33** (1996) 3297-3308.

9. V. Tvergaard, J. W. Hutchinson, On the toughness of ductile adhesion joints, *J. Mech. Phys. Solids,* **5** (1996) 789-800

10. Y. Wei, J. W. Hutchinson, Interface strength,work of adhesion and plasticity in the peel test, *Int. Journal of Fracture,* **93** (1998) 315-333.

11. I. Mohammed, and K. M. Liechti, Cohesive Zone Modeling of Crack Nucleation from Bimaterial Corners, *J. Mech. Phys. of Solids* **48** (2000) 735-764.

12. Z.-H. Jin., C. T. Sun., Cohesive fracture model based on necking, *Int. Journal of Fracture,* **134** (2005) 91-108.

13. Z.-H. Jin., C. T. Sun., Cohesive zone modeling of interface fracture in elastic bi-materials, *Eng. Frac. Mech.* **72** (2005) 1805-1817.

14. C. R. Chena., O. Kolednik., J. Heerense., F. D. Fischerf., Three-dimensional modeling of ductile crack growth: Cohesive zone parameters and crack tip triaxiality, *Eng. Frac. Mech.* **72** (2005) 2072-2094.

15. G. I. Brenblatt, Mathematical theory of equiblrium crack in brittle, *Adv. Appl. Mech.* Vol. 7, 1962

16. M. Lane., H. R. Dauskardt., Plasticity contribution to interface adhesion in thin film interconnect structures, *J. Mater. Res.* **15** (2000) 2758-2768.

17. J. R. Rice., A path independent integral an the approximate analysis of strain concentration by notches and cracks, *J. Appl. Mech.* (1968) 379-386

18. ABAQUS 6.5, *Analysis User's Manual*, Vol. 4, pp 18.5.1-18.5.6

19. T. Kitamura, H. Hirakata, Do Van Truong, Initiation of interface crack at free edge between thin films with weak stress singularity, *Thin Solid Films*, (under reviewing)

20. H. Hirakata, T. Kitamura, T. Kusano, Pre-cracking technique for fracture mechanics experiments along interface between thin film and substrate, *Engng. Fract. Mech.* **72** (2005) 1892-1904.

DỰ BÁO ĐỘ BỀN TÁCH LỚP BỀ MẶT GIỮA LỚP VẬT LIỆU MỎNG VÀ LỚP NỀN BẰNG MÔ HÌNH VÙNG KẾT DÍNH

Thiết bị vi điện tử bao gồm nhiều lớp vật liệu mỏng có chiều dày nano mét, và sự tách lớp giữa các lớp vật liệu đó thường xảy ra ở cạnh bề mặt nguyên do ứng suất kỳ dị ở cạnh bề mặt. Vì ứng suất kỳ dị ở cạnh bề mặt phụ thuộc vào hình dạng cạnh, do đó ta không thể sử dụng khái niệm cơ học phá huỷ để tính toán và so sánh độ bền tách lớp giữa các lớp vật liệu với những hình dạng khác nhau. Mục đích của bài báo này là dự báo sự tách lớp vật liệu ở cạnh tự do với những hình dạng tùy ý bằng việc sử dụng mô hình vùng kết dính. Hai thí nghiệm khác nhau được áp dụng đối với lớp kim loại mỏng vàng (Au) phủ trên lớp vật liệu nền silicon (Si) nhằm mục đích xác định luật kết dính của bề mặt. Cuối cùng, sự đúng đắn của phương pháp cũng được thảo luận.